

Tracing glacier changes since the 1960s

S. Thakuri et al.

Tracing glacier changes since the 1960s on the south slope of Mt. Everest (central Southern Himalaya) using optical satellite imagery

S. Thakuri^{1,3}, F. Salerno^{1,2}, C. Smiraglia³, T. Bolch^{4,5}, C. D'Agata³, G. Viviano¹, and G. Tartari¹

¹National Research Council, Water Research Institute (IRSA -CNR), Brugherio, Italy

²Ev-K2-CNR Committee, Via San Bernardino, 145, Bergamo 24126, Italy

³Department of Earth Sciences "Ardito Desio", University of Milan, Italy

⁴Department of Geography, University of Zurich, Switzerland

⁵Institute for Cartography, Technische Universität Dresden, Germany

Received: 1 September 2013 – Accepted: 26 October 2013 – Published: 8 November 2013

Correspondence to: S. Thakuri (thakuri@irsa.cnr.it)

Published by Copernicus Publications on behalf of the European Geosciences Union.

Title Page

Abstract

Introduction

Conclusions

References

Tables

Figures

◀

▶

◀

▶

Back

Close

Full Screen / Esc

Printer-friendly Version

Interactive Discussion



Abstract

We contribute to the debate on glacial shrinkage in the Himalaya by analyzing glaciers in southern slopes of Mt. Everest that are characterized by extensive debris coverage and the highest elevation in the world. In this paper, we make a complete analysis from 1962 to 2011, considering five intermediate periods using optical satellite imagery. We found an overall surface area shrinkage of $13.0 \pm 3\%$, an upward shift of 182 ± 9 m in snow-line altitude (SLA), a terminus retreat of 403 ± 9 m, and an increase of $17.6 \pm 3\%$ in debris coverage. The recession process of glaciers has been relentlessly continuous over the past fifty years. Furthermore, since early 1990s, we have observed an acceleration of the surface area shrinkage, which resulted in a median annual rate double that of the previous three decades (an increase from $0.27\% \text{ a}^{-1}$ to $0.46\% \text{ a}^{-1}$). Comparing the SLA over the same periods, it shifts upward with a velocity almost three times greater (from $2.2 \pm 0.5 \text{ m a}^{-1}$ to $6.1 \pm 0.9 \text{ m a}^{-1}$), which points to a worsening of the already negative mass balance of these glaciers. However, the increased recession velocity has only significantly affected glaciers with the largest sizes, which are located at higher altitudes and along the preferable south-oriented direction of the monsoons. Moreover, these glaciers present median upward shifts of the SLA that are double others; this finding leads to a hypothesis that Mt. Everest glaciers are shrinking, not only due to warming temperatures, but also as a result of weakening Asian monsoons registered over the last decades. We conclude that the shrinkage of these glaciers is less than that of others in the Himalayan range. Their position in higher elevations have surely reduced the impact of warming on these glaciers, but have not been excluded from a relentlessly continuous and slow recession process over the past fifty years.

Tracing glacier changes since the 1960s

S. Thakuri et al.

Title Page

Abstract

Introduction

Conclusions

References

Tables

Figures



Back

Close

Full Screen / Esc

Printer-friendly Version

Interactive Discussion



1 Introduction

The recent controversies concerning the possibly faster glacial shrinkage in the Himalaya than in any other part of the world (Cogley et al., 2010; Bagla, 2009) have focused global attention on necessity for a more comprehensive study in this region.

5 Current uncertainties are mainly attributed to a lack of measurements, both of glaciers and of climatic forcing agents (Bolch et al., 2012). The need for a fine-scale investigation is particularly evident on the south slope of Mt. Everest, which is one of the most heavily glaciated parts of the Himalaya. Glaciers here are characterized by abundant debris coverage, an effect that has often been neglected in predictions of future water
10 availability (Scherler et al., 2011; Salerno et al., 2012).

Some previous studies have discussed that debris-covered glaciers behave unlike clean glaciers (Nakawo et al., 1999; Scherler et al., 2011; Benn et al., 2012). More recently, Scherler et al. (2011) studied debris-covered glaciers around the Himalayan mountain range for a period of 2000–2008 and showed that heavy debris coverage influences terminus (Term) behaviors by stabilizing the terminus position change
15 (Δ Term). On the contrary, Kääb et al. (2012), in a comprehensive study on the glacier mass change from 2003–2008 in the Himalaya, suggested that debris-covered ice thins at a rate similar to that of exposed ice and indicated a need for further assessment of the role of debris mantles. Significant mass loss despite thick debris-cover was also
20 reported by Bolch et al. (2011), Nuimura et al. (2012) and Pieczonka et al. (2013).

We have decided to contribute to the international debate on glacier changes in the Himalaya by focusing our attention on the south slopes of Mt. Everest, whose peculiarities include extensive debris coverage and the highest elevation in the world. In this paper, we make a complete analysis of terminus retreat (Δ Term), surface area shrinkage (Δ Surf), shift of snow-line altitude (Δ SLA), and differences in debris coverage
25 (Δ DebrisCov) from 1962 to 2011 by analyzing five intermediate periods using optical satellite imagery, with the assistance of all available historical maps. The results are compared with those obtained in previous studies in this area and along the Himalaya

Tracing glacier changes since the 1960s

S. Thakuri et al.

Title Page

Abstract

Introduction

Conclusions

References

Tables

Figures



Back

Close

Full Screen / Esc

Printer-friendly Version

Interactive Discussion



range. We conclude by attempting to link the observed impacts with the climate change drivers.

2 Study area

The current study is focused on the Mt. Everest region, and in particular in the Sagarmatha (Mt. Everest) National Park (SNP) (27.75° to 28.11° N; 85.98° to 86.51° E) that lies in the eastern Nepal (central Southern Himalaya) (Fig. 1a). The park area (1148 km²), extending from an elevation of 2845 m at Jorsale to 8848 m a.s.l., covers the upper catchment of Dudh Khosi river. Land cover classification shows that almost one-third of the territory is characterized by glaciers and ice cover, while less than 10 % of the park area is forested (Salerno et al., 2010a). The SNP is the world's highest protected area with over 30 000 tourists in 2008 (Salerno et al., 2010b; Salerno et al., 2013). This region is one of the heavily glacierized parts of the Himalaya with the presence of many debris-covered glaciers: those glaciers where the ablation zone is almost entirely covered by surface debris (Fig. 1b) (Scherler et al., 2011).

Several debris-covered glaciers have stagnant ice at their termini (Bolch et al., 2008b). However, these glaciers have potential to develop widespread melting ponds and build up moraine-dammed lakes (Bolch et al., 2008b; Quincey et al., 2009). Gardelle et al. (2011) note that the southern side of Mt. Everest is the region that is most characterized by glacial lakes in the Hindu Kush Himalaya. Salerno et al. (2012) reported a total of 624 lakes in the park including 17 proglacial lakes, 437 supraglacial lakes and 170 unconnected lakes. In general, they observed that supraglacial lakes occupy from approximately 0.3 % to 2 % of glacier downstream surfaces.

The glacier hypsometric curve plotted, using the glacier outlines of 2011 and the Advanced Spaceborne Thermal Emission and Reflection Radiometer-Global Digital Elevation Model Version 2 (ASTER GDEM) indicates that the glacier surfaces are distributed from around 4300 m to above 8000 m a.s.l. with more than 75 % glacier surfaces lying between 5000 m and 6500 m a.s.l. (Fig. 1c); the median elevation is

Tracing glacier changes since the 1960s

S. Thakuri et al.

Title Page

Abstract

Introduction

Conclusions

References

Tables

Figures



Back

Close

Full Screen / Esc

Printer-friendly Version

Interactive Discussion



Tracing glacier changes since the 1960s

S. Thakuri et al.

Title Page

Abstract

Introduction

Conclusions

References

Tables

Figures

◀

▶

◀

▶

Back

Close

Full Screen / Esc

Printer-friendly Version

Interactive Discussion

5664 m a.s.l. These glaciers are identified as the summer-accumulation type fed mainly by summer precipitation from the South Asian monsoon system, whereas the winter precipitation caused by mid-latitude westerly wind is minimal (Ageta and Fujita, 1996; Tartari et al., 2002). The prevailing axis of the monsoons is southern and south-western (Rao, 1976; Müller, 1980; Ichianagi et al., 2007). Based on the meteorological observations at the Pyramid Laboratory Observatory (5050 m a.s.l.), the mean annual air temperature is $-2.5 \pm 0.5^\circ\text{C}$. In summer (June–September), air temperature is typically above 0°C , the maximum occurs in July, and shows a typical variation associated with cloudiness. In contrast, thermal range is very high during winter owing to less cloudy conditions. In winter, the maximum daily temperature is usually below 0°C , especially in February, the coldest month. Mean total annual precipitation is $516 \pm 75 \text{ mm a}^{-1}$, with about 88% of the annual amount recorded during the summer months (June–September). The vertical gradients of temperature, solar radiation, and precipitation have been calculated using 5 meteorological stations located in the SNP ranging from 2660 to 5600 m a.s.l. and managed by Ev-K2-CNR Committee (Ueno et al., 2008). We found a lapse rate of $-0.0059^\circ\text{C m}^{-1}$, a solar radiation gradient of $+0.024 \text{ W m}^{-2} \text{ m}^{-1}$, valid only for pre- and post-monsoon months, while the monsoon period is affected by high cloud cover. Above 4000 m a.s.l. the precipitation starts decreasing ($-0.017 \text{ mm}[\text{month}] \text{ m}^{-1}$).

3 Data and methods

3.1 Data sources

The analyses of ΔTerm , ΔSurf , ΔSLA and $\Delta\text{DebrisCov}$ of Mt. Everest glaciers were performed from 1962 to 2011 using satellite imagery, with the assistance of all available historical maps (Table 1). We analyzed the glacier changes within 5 periods: 1962–1975, 1975–1992, 1992–2000, 2000–2008 and 2008–2011.

Tracing glacier changes since the 1960s

S. Thakuri et al.

Title Page

Abstract

Introduction

Conclusions

References

Tables

Figures

◀

▶

◀

▶

Back

Close

Full Screen / Esc

Printer-friendly Version

Interactive Discussion

All satellite data were acquired after the monsoon season during the period of October–December. These images are characterized by low cloud cover and correspond to time just after the end of the snow accumulation and ablation period for that year; this allows for homogeneous comparisons (Paul et al., 2009). The declassified Corona KH-4 (hereafter Corona-62) was used as a main data source for the base year of the analysis (1962). The Khumbu Himal map of late 1950s (hereafter KHmap-50s) and the topographic map of the Indian Survey of 1963 (hereafter TISmap-63) were used to complement the results achieved using Corona-62 since the Corona-62 had the complex image geometry and absence of satellite camera specification for its rectification. The KHmap-50s has clear glacier boundaries, but the TISmap-63 has less discernible glacier outlines; thus, the first map was used for analysis related to Δ Surf, Δ Term and Δ SLA, while use of the TISmap-63 was limited to Δ Term. The Corona KH-4B (Corona-70) image covers only a small portion of the southern part of the study area. Therefore, the Landsat MSS (1975) (Landsat-75) was used as the main data source, although its pixel resolution is significantly lower. Moreover, we compared the 1992 Landsat TM scene (Landsat-92) with the official topographic map of Nepal from same year (OTNmap-92). Concerning the more recent years, we used Landsat ETM+ scenes from 2000 (Landsat-00), 2011 (Landsat-11), and an ALOS AVNIR-2 scene (ALOS-08).

The ASTER GDEM was used to derive the glacier morphological features (slope, aspect, elevation); the digital elevation model (DEM) tiles for the Mt. Everest region were downloaded from <http://gdem.ersdac.jspacesystems.or.jp>. The vertical accuracy is ~ 20 m, and horizontal accuracy is ~ 30 m (<http://www.jspacesystems.or.jp/ersdac/GDEM/E/4.html>). We decided to use the ASTER GDEM instead of the Shuttle Radar Topography Mission (SRTM) DEM considering the higher resolution (30 m and 90 m, respectively) and the large data gaps of the SRTM DEM in this study area (Bolch et al., 2011). Furthermore the ASTER GDEM shows better performance in mountain terrains (Frey et al., 2012).

3.2 Gap fill and pansharpening of Landsat-11

The problem of the Scan Line Corrector failure (SLC-off) gap (Parkinson et al., 2006) in Landsat-11 was corrected using the IDL (Interactive Data Language) Extension-gap fill tool in ENVI[®] software that uses a local linear histogram matching algorithm in the application of another image from same year (Chen et al., 2011). The effect of the SLC-off gap in our study area can be assumed to be minimal due to the central location of our study area in the Landsat scene. More than 1/3 of our study area was not affected by the data gaps and the glaciers' boundaries were manually delineated taking the interpolation uncertainties into account. The Landsat-11 multispectral bands (30 m) were pan-sharpened for visual improvement (Rodriguez-Galiano et al., 2012) using the panchromatic band (15 m) acquired by same satellite and on the same date.

3.3 Data registration

All of the imagery and maps were co-registered in the same coordinate system of WGS 1984 UTM Zone 45N. The Landsat scenes were provided in standard terrain-corrected level (Level 1T) with the use of ground control points (GCPs) and necessary elevation data (<https://earthexplorer.usgs.gov>). The ALOS-08 image used here was orthorectified and corrected for atmospheric effects in Salerno et al. (2012). The Corona images were co-registered and rectified through the polynomial transformation and spline adjustment using more than 120 known GCPs obtained from the image, including mountain peaks, river crossings, and identifiable rocks (Grosse et al., 2005; Lorenz, 2004). The polynomial transformation uses a least squares fitting algorithm and ensures the global accuracy of images (Rosenholm and Akerman, 1998) but does not guarantee local accuracy, whereas the spline adjustment improves for local accuracy, which is based on a piecewise polynomial that maintains continuity and smoothness between adjacent polynomials (Kresse and Danko, 2011). The images were resampled using the nearest neighbor method to new pixel size.

Tracing glacier changes since the 1960s

S. Thakuri et al.

Title Page

Abstract

Introduction

Conclusions

References

Tables

Figures



Back

Close

Full Screen / Esc

Printer-friendly Version

Interactive Discussion



3.4 Interpretation and mapping of glacier features

The automated glacier mapping from satellite imagery is hindered by DebrisCov (Racoviteanu et al., 2008). Though the automatic methods are intended for mapping these types of glaciers, the results are less accurate and need intensive manual post-correction (Paul et al., 2004; Bhambri et al., 2011). In this study, the glacier outlines were manually delineated using an on-screen digitizing method based on visual interpretation and false-color composite (FCC) developed from multispectral bands and assisted by the DEM (Fig. 2a and b). In the ablation part of the glacier, due to the presence of a debris mantle, the delineation of the outline was performed by identifying lateral and frontal moraine and using the thermal band for the Landsat TM and ETM images. The presence of multispectral bands allowed us to develop the band ratio (TM4/TM5) images, which provided good information for delineating the glaciers in the shaded region due to topographic effects, and the normalized difference snow index images (Paul et al., 2002) to obtain a clear vision of snow and ice portion that assisted in the manual digitization.

For the Δ Term calculation, a band of stripes with a distance of 50 m between each stripe in the band was drawn parallel to the main flow direction of the glacier (Fig. 2), and the Δ Term was calculated as the average length from the intersection of the stripes with the glacier outlines (cf. Koblet et al., 2010; Bhambri et al., 2012).

The snow lines were retrieved manually from each satellite image and map. The snow lines in the images were distinguished as the boundary between the bright white snow and the darker ice by visual interpretation and using FCC (Karpilo, 2009). The kinematics “Hess method” (Hess, 1904) was used to identify the snow line in the KHmap-50s, which involves the delineation of the boundary between the accumulation and ablation zone in a glacier using the inflection of elevation contour lines on the topographic map (Leonard and Fountain, 2003). Then, the SLA, as a measure of ELA, was calculated as the average altitude of the identified snow line using the ASTER GDEM. The SLA derived from the “Hess method” for the map represents the long-

Tracing glacier changes since the 1960s

S. Thakuri et al.

Title Page

Abstract

Introduction

Conclusions

References

Tables

Figures



Back

Close

Full Screen / Esc

Printer-friendly Version

Interactive Discussion



Tracing glacier changes since the 1960s

S. Thakuri et al.

Title Page

Abstract

Introduction

Conclusions

References

Tables

Figures

◀

▶

◀

▶

Back

Close

Full Screen / Esc

Printer-friendly Version

Interactive Discussion



In this study, the uncertainty of measurement ranges from 6 to 30 m for Δ Term and from 6 to 30 m for Δ SLA. In both cases, as discussed below and shown in Fig. 3 and Table 2, the magnitude of the uncertainty is relatively low if compared with the observed changes, indicating good accuracy of the results. However, the errors associated with Δ Surf and Δ DebrisCov range from approximately 2 to 10 % for both of variables. In particular, Fig. 3 and Table 2 indicate that until early 1990s, this uncertainty, due to low sensor resolution, is high and needs to be carefully considered in the change evaluations.

3.6 The ELA-Climate model

To evaluate the role of climatic drivers in the Δ SLA, we used the simple *ELA-Climate model* by Kuhn (1981) (Hooke, 2005). This model has been widely used in the European Alps (Kerschner, 1997), New Zealand (Hoelzle et al., 2007) and the Himalaya (Kayastha and Harrison, 2008) to estimate the climate drivers changes required for explaining the observed SLA change. The model (Eq. 1) requires temperature lapse rate, mass balance and radiation gradients, latent heat of fusion and length of melting season.

The model is expressed as

$$\frac{\partial b_w}{\partial z} \Delta h + \delta b_w = \frac{T}{L} \left[\frac{\partial R}{\partial z} \Delta h + \delta R + \gamma \left(\frac{\partial T_a}{\partial z} \Delta h + \delta T_a \right) \right] \quad (1)$$

where Δh = an observed change in ELA (m); T = length of melting season (d); L = Latent heat of fusion (kJ kg^{-1}); γ = constant ($\text{MJ m}^{-2} \text{d}^{-1} \text{K}^{-1}$); $\partial b_w / \partial z$ = mass balance gradient ($\text{kg m}^{-2} \text{m}^{-1}$); $\partial T_a / \partial z$ = temperature lapse rate (K m^{-1}); $\partial R / \partial z$ = net radiation gradient ($\text{MJ m}^{-2} \text{m}^{-1} \text{d}^{-1}$); δT_a = bias in air temperature (K); δb_w = bias in mass balance (kg m^{-2}); δR = bias in net radiation ($\text{MJ m}^{-2} \text{d}^{-1}$). We applied the model using the temperature lapse rate and the net radiation gradient calculated for this case study as described above, the mass balance gradient of $5 \pm 1 \text{ mm m}^{-1}$ w.e. provided by

Fujita et al. (2006), $T = 100$ d; $L = 334$ kJ kg⁻¹, $\gamma = 1.7$ MJ m⁻² d⁻¹ K⁻¹ as described in Kuhn (1981).

3.7 Statistical analysis

The normality of the data is tested using the Shapiro–Wilk test. The null hypothesis for the Shapiro–Wilk test is that samples x_1, x_2, \dots, x_n belong to a normally distributed population. If the p value (p) > 0.05 , we consider the series to be normally distributed; otherwise, it is not normal (Shapiro and Wilk, 1965). We used the paired t test for comparing the means of two series. The null hypothesis is that the difference between paired observations is zero ($p < 0.05$) (Walford, 2011). If the series were not normal, we first used a log transformation to apply the paired t test for a normally distributed series. All tests are implemented in the R software environment.

4 Results

Table 2 provides a general summary of the changes that occurred from 1962 to 2011. Our main findings, however, are visualized in Fig. 3, which has been subdivided into 4 sections (a–d), corresponding to four selected indicators of change (Term, Surf, SLA and DebrisCov). The spatial differences are presented on the right side of each section, and the temporal changes are shown on the left side. On the left side, in the upper panel of each section, the box plots show the annual rates of change for the analyzed period, while the cumulative changes and their associated uncertainties are presented in the lower panels. All data presented and discussed in this paper are reported in Table S1 of Supplement.

4.1 Glacier terminus position change

Overall, from 1962 to 2011, the Mt. Everest glaciers experienced a Δ Term of 403 ± 9 m ($\sigma = 533$ m) (Fig. 3a2 and Table 2) as the mean retreat (301 ± 9 m as median), cor-

Tracing glacier changes since the 1960s

S. Thakuri et al.

Title Page

Abstract

Introduction

Conclusions

References

Tables

Figures



Back

Close

Full Screen / Esc

Printer-friendly Version

Interactive Discussion



a closer mean retreat to the Corona-62 ($8.2 \pm 0.2 \text{ ma}^{-1}$) than to the TISmap-63 ($13.3 \pm 2.6 \text{ ma}^{-1}$), which seems to overestimate the ΔTerm .

4.2 Glacier surface area change

Overall, from 1962 to 2011, the Mt. Everest glaciers experienced a ΔSurf of $52.8 \pm 11.0 \text{ km}^2$ (from 404.6 to 351.8 km^2), corresponding to an overall change of $13.0 \pm 3.1 \%$ ($0.27 \pm 0.06 \%$ a^{-1}) (Fig. 3b2 and Table 2). The mean annual shrinkage rate calculated for each glacier in the period from 1962–2011 was $0.51 \pm 0.06 \%$ a^{-1} ($\sigma = 0.38$), and the median rate was $0.42 \pm 0.06 \%$ a^{-1} (Fig. 3b1). By testing the annual shrinkage rate (Shapiro–Wilk test) of each glacier in each observed period, we observed (similar to the terminus retreat) that it was never normally distributed (see box plots in Fig. 3b1). Therefore, in this case as well, we consider it to be more representative of change in the median values.

We can observe a continuous shrinkage since 1960s that appears to have accelerated in the last years (Fig. 3b2). In fact, the median annual shrinkage rate was 0.27% a^{-1} in 1962–1975 and has increased to the rate of loss of 0.76% a^{-1} , nearly 3 times greater (Fig. 3b1). We thus tested these trend properties using same procedure that we had adopted for evaluating the terminus retreats. In this case, we again first provided a log transformation of the series. We observed that the surface area shrinkage of each period was always significantly different from zero. The weakest significance was found in the 1962–1975 period. In fact, Fig. 3b2 and Table 2 show lower observed surface change (1.7%) for this period, which, although significant, is associated with the highest uncertainty (9.7%). However, in evaluating the possible acceleration of the surface area losses, we found significant differences ($p = 0.02$) between the annual shrinkage rates of the 1962–1992 period (median $0.27 \pm 0.13 \%$ a^{-1}) and the 1992–2011 period (median $0.46 \pm 0.25 \%$ a^{-1}), indicating that for the 1992–2011 period, each glacier is retreating at nearly double the rate than the previous period, on average.

Tracing glacier changes since the 1960s

S. Thakuri et al.

Title Page

Abstract

Introduction

Conclusions

References

Tables

Figures



Back

Close

Full Screen / Esc

Printer-friendly Version

Interactive Discussion



Tracing glacier changes since the 1960s

S. Thakuri et al.

[Title Page](#)[Abstract](#)[Introduction](#)[Conclusions](#)[References](#)[Tables](#)[Figures](#)[Back](#)[Close](#)[Full Screen / Esc](#)[Printer-friendly Version](#)[Interactive Discussion](#)

The shrinkage observed in the first period (1962–1975) using Corona-62 and Landsat-75 was sustained using different data sources, as described in the methods section and shown in Table 1. Comparing the KHmap-50s with the Landsat-75, we obtain a glacier area loss of $0.22 \pm 0.64 \% a^{-1}$, which is very close to the value obtained using Corona-62 ($0.27 \% a^{-1}$). Moreover, for some glaciers, we were able to substitute high resolution Corona-70 with Landsat-75 to provide information about the accuracy of the Landsat data. The comparison of Corona-62 and Corona-70 provided a mean rate of $0.26 \% a^{-1}$, confirming that between late 1950s and early 1970s, the glacier surface losses were very small.

Figure 3b3 represents a distinct spatial pattern of glacier $\Delta Surf$. All of the glaciers experienced Surf losses between 1962 and 2011. However, the southern glaciers shrank more than the northern glaciers.

4.3 Snow-line altitude change

Overall, from 1962 to 2011, the SLA of Mt. Everest glaciers shifted upward by 182 ± 9 m ($\sigma = 114$) from 5289 m to 5471 m a.s.l.; this increase corresponds to a mean annual rate of 3.7 ± 0.2 m a^{-1} ($\sigma = 2.3$) (Fig. 3c1, c2 and Table 2). The distribution of the shift annual rate of the SLA in all of the observed periods is in this case normal (Shapiro–Wilk test; see box plots in Fig. 3c1). Therefore, the mean values are suitable for describing the ΔSLA .

In Fig. 3c2, the overall trend in ΔSLA shows a continuous upward shift in the last 50 yr. In fact, in Fig. 3c1, we can observe that the mean annual upward rate of the SLA was 2.0 ± 2.3 m a^{-1} in 1962–1975 and achieved the highest shift rate of 10.6 ± 3.0 m a^{-1} in the recent years. In this case, we tested the possible continuity and acceleration of trend following the same procedure applied above. We observed a statistically significant upward shift of the SLA ($p = 0.02$), except during the first period of 1962–1975. Moreover, we found significant differences ($p < 0.001$) in the annual upward shift of the SLA between periods 1962–1992 (mean = 2.2 ± 0.5 m a^{-1}) and 1992–2011 (mean = 6.1 ± 0.9 m a^{-1}).

Figure 3c3 represents the spatial distribution of the SLA for the overall 1962–2011 period. In this case, the spatial pattern is not distinct. The glaciers with the minimum and maximum SLA in 2011 are Cholo (5152 m.a.s.l.) and Imja (5742 m), respectively.

Furthermore, as mentioned above, we calculated the SLA using the KHmap-50s with the “Hess method,” which provides an average position of the average snow line for the 1950s. We observed the SLA at 5272 m.a.s.l., which is not very different from the SLA at 5289 m.a.s.l., as derived from Corona-62.

4.4 Glacier debris-covered area change

Overall, the debris-covered area has increased by $17.6 \pm 3.0\%$ ($0.36 \pm 0.06\% \text{a}^{-1}$) (Fig. 3d2 and Table 2) from 1962 to 2011 (Fig. 4a1 and Table 2). The mean annual increase rate calculated for each glacier in the 1962–2011 period is $0.28 \pm 0.06\% \text{a}^{-1}$ ($\sigma = 0.34$), and the median rate is $0.21 \pm 0.06\% \text{a}^{-1}$ (Fig. 3d1). The debris-covered area was approximately 24.5% of the total glacier area in 1962 and 32.0% in 2011. Testing the annual DebrisCov change rate with the Shapiro–Wilk test, we observed that the increase of the debris-covered area is not normally distributed among all glaciers (Fig. 3c1). Therefore, we also consider the median values to be more representative of change in the case of $\Delta\text{DebrisCov}$.

In Fig. 3a2, we present the overall $\Delta\text{DebrisCov}$ trend, which indicates a general continuous increase of debris cover area over the last 50 yr. We observed that the debris cover increase began to be statistically significant for each glacier only after 2000 ($p < 0.01$). However, in evaluating the possible acceleration, we found no significant differences among the annual rates of changes ($p > 0.1$). The result of this test can be observed in Fig. 3d1, which considers the distribution of median annual rates. Since 2000, the debris cover rates appear to be decreasing, although not significantly.

In Fig. 3d3, we can observe the spatial distribution of the debris-covered area (%) in the overall period of analysis of 1962–2011. We observe that the glaciers experienced an overall increase in the debris-covered area, except the glaciers Imja, Kdu_gr125, Langdak and Langmuche for which local effects could have played an important role.

Tracing glacier changes since the 1960s

S. Thakuri et al.

Title Page

Abstract

Introduction

Conclusions

References

Tables

Figures



Back

Close

Full Screen / Esc

Printer-friendly Version

Interactive Discussion



5 Discussion

5.1 Comparison among terminus position change, surface shrinkage and the relevant mass budget observations

Mass budget measurements are the main index used for climate change impact studies on glaciers, as used by Fujita et al. (2006), Bolch et al. (2011), Nuimura et al. (2012), and Gardelle et al. (2013) as this index can be directly linked to climate while length and area change show a delayed signal (Bolch et al., 2012). However, conducting mass-balance measurements is not a trivial task, due to the technical requirements and practical constraints (Bolch et al., 2012); these measurements are thus not often used in extensive studies. Most of the authors, in fact, analyze Term and Surf (Bolch et al., 2012; Yao et al., 2012; Kulkarni et al., 2011; Scherler et al., 2011). However, we need to consider the limitations of these variables especially for debris-covered glaciers, which experience more down-wasting than shrinkage (Bolch et al., 2011; Tennant et al., 2012). In this regard, we decided to compare our findings in terms of ΔTerm , ΔSurf and ΔSLA with the corresponding mass budget information provided by other authors to evaluate whether these factors are suitable indices in this context. We used the mass budget derived using geodetic methods for 10 glaciers located in our study area, which are provided by Bolch et al. (2011) and Nuimura et al. (2012). Bolch et al. (2011) gives mass loss rates of $0.21 \pm 0.10 \text{ m a}^{-1}$ and $0.79 \pm 0.52 \text{ m a}^{-1}$ w.e. for the 1970–2002 and 2002–2007 periods, respectively, while Nuimura et al. (2012) reported mass loss rates of $0.07 \pm 0.20 \text{ m a}^{-1}$ and $0.45 \pm 0.60 \text{ m a}^{-1}$ w.e. for the 1992–2000 and 2000–2008 periods, respectively (Fig. 4). Both studies (Bolch et al., 2011; Nuimura et al., 2012) find a higher rate of mass loss for the last decade. Recently Gardelle et al. (2013) provided the mass balance value $0.26 \pm 0.09 \text{ m a}^{-1}$ w.e. for 1999–2011 for a wider glacier area in the region (1461 km^2).

Figure 4 shows that, for the same glaciers, we observed a ΔTerm that was slightly higher in the second period (2000–2011) than in the previous one (1992–2000), while the ΔSurf and the ΔSLA were both approximately 4 times higher in the last decade,

Tracing glacier changes since the 1960s

S. Thakuri et al.

Title Page

Abstract

Introduction

Conclusions

References

Tables

Figures

◀

▶

◀

▶

Back

Close

Full Screen / Esc

Printer-friendly Version

Interactive Discussion



as observed using mass budget data. This comparison shows that, for this region, the glacier surface shrinkage and the shift of snow-line altitude (i.e., the shift of late summer snow line) can be considered suitable indicators for a broad description of glacial response to the recent climate change. Differently, Gardelle et al. (2013) seems to underestimate the mass loss in the last decade.

5.2 Comparison with other parts of Himalaya

Bolch et al. (2012) recently noted that length and surface area changes suggest that most Himalayan glaciers have been retreating since the mid-19th century. These measurements indicate that the mass budget over large parts of the Himalaya has been negative in this period and the rate of loss increased after approximately 1995, although the spatio-temporal variability is high. We confirm in the subsequent session, an accelerated rate of shrinkage since the early 1990s even for the glaciers on the south slope of Mt. Everest. However, we specify that Bolch et al. (2008a) found, for few selected glacier in this region, a lower shrinkage ($0.12\% \text{ a}^{-1}$) between the 2001–2005 period compared to the 1992–2001 period ($0.25\% \text{ a}^{-1}$) probably due to a low sample representativeness, as explained by the same authors.

Yao et al. (2012) reported the glacier status over the past 30 yr in the Tibetan Plateau and surroundings. Systematic differences in glacier status are apparent from region to region, with the greatest reduction in glacial length and area and the most negative mass balance occurring in the Himalaya (excluding Karakorum). The shrinkage generally decreases from the Himalaya to the continental interior, and it is most pronounced in the southeastern Himalayan region.

As already mentioned, the south slope of Mt. Everest is one of the heavily glacierized parts of the Himalaya (Scherler et al., 2011), and it thus is important to make a more extensive comparison between the behavior of glaciers here and those in rest of the Himalaya. We analyzed 29 glaciers in this area from 1962 to 2011 using all available data sources. Yao et al. (2012) considered only 3 benchmark glaciers in Nepal for evaluating the Term retreat during the 1974–1999 period and the same glaciers analyzed

Tracing glacier changes since the 1960s

S. Thakuri et al.

Title Page

Abstract

Introduction

Conclusions

References

Tables

Figures

◀

▶

◀

▶

Back

Close

Full Screen / Esc

Printer-friendly Version

Interactive Discussion



here (Khosi Basin) for evaluating the Surf shrinkage, but for a shorter period (1976–2000) than in the present study. Yao et al. (2012) reported a ΔTerm of 6.9 m a^{-1} based on the 3 glaciers; for a similar period (1975–2000), we calculated a median retreat of $4.4 \pm 0.8 \text{ m a}^{-1}$ for all 29 glaciers and a median retreat of $6.1 \pm 0.2 \text{ m a}^{-1}$ during the 1962–2011 period. Concerning the Surf shrinkage, Yao et al. (2012) reported a decrease of $0.15 \% \text{ a}^{-1}$, while during a similar period (1975–2000), we observed a shrinkage of $0.25 \pm 0.4 \% \text{ a}^{-1}$. We can observe that although the retreat rates are comparable between the studies, with regards to ΔSurf , we observed a greater shrinkage; this difference could be because both satellites used in 1975 and 1976 (Landsat MSS) had a broad resolution (60 m) leading to a large uncertainty in the estimates and, hence the studies are in line taking the uncertainty into account.

Moreover, we point out that the present study corresponds to zone III of the analysis of Yao et al.'s (2012), defined by the authors as central Himalaya and including both the north (Tibet) and south (Nepal) slopes of the Himalayan range, represented by the Mt. Qomolangma National Nature Preserve and the Khosi Basin, respectively. The average retreat and shrinkage rates for zone III have been established by the authors at 6.3 m a^{-1} and $0.41 \% \text{ a}^{-1}$, respectively. However, the glacier behavior is not homogeneous in central Himalaya, so this mean loses significance, particularly considering the different shrinkages observed for the northern and southern parts. In fact, according to Nie et al. (2010) and as reported by Yao et al. (2012), the shrinkage rate is $0.50 \% \text{ a}^{-1}$ (1976–2006) in the north; during the same period in the south, the shrinkage rate is about half that, according to the present study, and one third of that, according to Yao et al. (2012). Likewise, a shrinkage of $0.3 \% \text{ a}^{-1}$ for the 1974–2008 period was provided by Ye et al. (2009) on the northern side and $0.15 \% \text{ a}^{-1}$ for the 1950s–1992 period (Salerno et al., 2008) and $0.12 \% \text{ a}^{-1}$ for selected glaciers for the 1962–2005 period (Bolch et al., 2008a), both located in the southern side. Therefore, to explore possible differences in the surroundings of the south slopes of Mt. Everest, we decided to separately consider the north and south parts of Central, Western and Eastern Himalaya (CH, WH, and EH, respectively, with the suffixes -N and -S). Following this scheme, the

present case study and all of Nepal are located in CH-S. Evidence from the Tibetan Plateau (TP) is presented separately (Fig. 1a).

Figure 5 reports the most recent impact studies on Himalayan glaciers concerning both the terminus retreat (Fig. 5a) and the shrinkage (Fig. 5b). We can easily observe that the CH-S, in terms of both ΔTerm and ΔSurf , registered the lowest changes of the entire Himalayan range. The lower changes in Term and Surf observed in CH-S region, compared with the other parts of the Himalaya and TP, are related both to the abundance of DebrisCov (Scherler et al., 2011; Bolch et al., 2012) and to the altitude of these glaciers. Scherler et al. (2011) defined the southern central Himalaya as the region with the glaciers that contain the highest debris coverage ($\sim 36\%$) and considered the abundance of debris coverage to be a significant factor in reducing the melt rate of these glaciers, preserving their surfaces from further recession. However, of no less importance is the altitude of these glaciers. In fact, as reported by Bolch et al. (2012), with an elevation of 5600 m a.s.l., the highest glaciers of the Himalayan range are located in CH. On the south slope of Mt. Everest, the glacier elevation weighted by surface area is 5664 m a.s.l. Therefore, it is indisputable that the summit of the world has preserved these glaciers from excessive melting better than in the other parts of the Himalaya.

5.3 Snow-line altitude change and climate relation

Bolch et al. (2012), considering the mean elevation as a rough proxy for the ELA, reported an ELA of about 5600 m a.s.l. in CH. For the south slope of the Mt. Everest region, Owen and Benn (2005) indicated an elevation of 5200 m a.s.l. for the 1980s, while Asahi (2010) noted an altitude of 5400 m a.s.l. in the early 1990s. In this study, comparing the same years, we observed a SLA position of 5315 m a.s.l. in 1975 and 5355 m a.s.l. in 1992, corresponding to a lower shift. Kayastha and Harrison (2008) observed an upward of ELA by $0.9 \pm 1.1 \text{ m a}^{-1}$ ($29 \pm 35 \text{ m}$) during the 1959–1992 period using the toe-to-headwall altitude ratio (THAR) method with TISmap-63 and the aerial photos of 1992, from which the OTNmap-92 was delineated. In a comparable period (1962–1992), we calculated an upward shift of SLA by $2.2 \pm 0.4 \text{ m a}^{-1}$ ($66 \pm 11 \text{ m}$) based

Tracing glacier changes since the 1960s

S. Thakuri et al.

Title Page

Abstract

Introduction

Conclusions

References

Tables

Figures

◀

▶

◀

▶

Back

Close

Full Screen / Esc

Printer-friendly Version

Interactive Discussion



on satellite data. The difference between the calculation of Kayastha and Harisson (2008) and our calculation is mainly due to different methodologies applied and the data set used. Surely, if a suitable scene is available, the SLA derived directly from the satellite imagery is more representative of a specific year than the map-based estimation.

The SLA trend qualitatively indicates the mass-balance variation of glaciers (Chinn et al., 2005). Variations in SLA derived from satellite imagery can be used as a proxy for providing indications of local climate variability (Fujita and Nuimura, 2011; McFadden et al., 2011; Rabatel et al., 2012). In this case study, the SLA is significantly moving upwards, with an accelerated rate after 1992, indicating that the glaciers in this region are experiencing an increasingly negative mass balance as it is confirmed with the mass down-wasting observations of Bolch et al. (2011) and Nuimura et al. (2012) (Fig. 4). The observed upward shift the of snow line could be interpreted as a direct response to high-temperature events, reduced precipitation, or increased solar radiation (Hooke, 2005). To evaluate the role of climatic drivers in the Δ SLA, we used the simple ELA-Climate model by Kuhn (1981) (Hooke 2005). Using this model, we estimated that for the observed 182 m upward shift of SLA in the 1962–2011 period, a temperature increase of 1.1 °C, a precipitation decrease of 543 mm or a solar imbalance increase of 1.8 MJ m⁻² d⁻¹ is required. By reacting to this climate perturbation, the SLA shifted by 182 m upward.

Concerning the temperatures, on the south slope of Mt. Everest, Diodato et al. (2012) established the longest temperature series (1901–2009) for this high elevation area, taking advantage of both land data obtained from the “Pyramid” meteorological observatory (5050 m) for the 1994–2005 period and gridded temperature data for extending the time series. They observed an increasing trend of 0.01 °C a⁻¹ in the last century (+0.9 °C), which can be attributed mainly to the 1980–2008 period (0.03 °C a⁻¹, +0.8 °C). Likewise, Lami et al. (2010), using only the land data from the “Pyramid” stations (5050 m) for the 1992–2008 period, reported an increasing trend of 0.04 °C a⁻¹ (+0.7 °C). Kattel and Yao (2013) in the southern central Himalaya, observed an increas-

Tracing glacier changes since the 1960s

S. Thakuri et al.

Title Page

Abstract

Introduction

Conclusions

References

Tables

Figures

◀

▶

◀

▶

Back

Close

Full Screen / Esc

Printer-friendly Version

Interactive Discussion



using the Global Precipitation Climatology Project (GPCP) data, the Asian monsoon lost 173 mm in this region for the 1979–2010 period, with a real decreasing trend starting from the early 1990s (mean value between grid 9 and 11 in Fig. S18). We have already noted that we would have recorded a decrease of 543 mm if the only factor responsible for the higher SLA were the precipitation. Current knowledge shows that precipitation can be held responsible for approximately 30 % of the negative balance of glaciers in the study region (e.g., Yao et al., 2012; Palazzi et al., 2013).

Establishing the influence of solar radiation on the negative mass balance of these glaciers is much more difficult considering the complete global lack of long-term measurements of this variable at high elevations. For the Northern Hemisphere, Wild et al. (2005) reported a general decrease of sunlight over land surfaces, using the popular expression “global dimming,” on the order of 2 to $5 \text{ W m}^{-2} \text{ decade}^{-1}$ (1960–1990 period), corresponding to a decline of 4 % to 9 %. A partial recovery (“global brightening”) has been registered more recently (1986–2000) at many locations ($2.2 \text{ W m}^{-2} \text{ decade}^{-1}$, corresponding to a rise of 2 %). According to Wild (2009), changes in solar radiation can be due to (1) changes in cloud cover and optical properties, (2) changes in water vapor, and (3) changes in the mass and optical properties of aerosols. However, sensitivity studies indicate that considerable changes in water vapor would be necessary to explain the observed solar radiation trends, while changes in cloud and aerosol characteristics are the dominant factors (Wild, 1997). Since early 1990s, reduced emissions have been registered in Asia, with a resulting decline of aerosol concentrations (Streets et al., 2009). This trend reversal in aerosol levels fits the general picture of a widespread transition from dimming to brightening (Ramanathan et al., 2005). Furthermore, the weakness of the monsoon could correspond to minor cloud coverage; both factors are favorable for hypotheses of an increase in solar radiation in this region. Furthermore, the aerosol–cloud interactions cause an amplification of dimming and brightening trends in pristine environments (Kaufman et al., 2005; Wild, 2009). The average solar radiation at the 5050 m elevation is $12.4 \text{ MJ m}^{-2} \text{ d}^{-1}$ (143.5 W m^{-2}) (Tartari et al., 2002). The increase of nearly 15 % ($1.7 \text{ MJ m}^{-2} \text{ d}^{-1}$ or

Tracing glacier changes since the 1960s

S. Thakuri et al.

Title Page

Abstract

Introduction

Conclusions

References

Tables

Figures

◀

▶

◀

▶

Back

Close

Full Screen / Esc

Printer-friendly Version

Interactive Discussion



19.7 W m⁻²) of solar radiation is large if compared with the 2 % of global rise reported for the recent years, but it cannot be excluded, according to Kaufman et al. (2005) and Wild (2009), that the aerosol–cloud interactions cause an amplification of dimming and brightening trends in pristine environments.

5.4 Acceleration of the recession process

We observed clear signs of glacier changes since 1960s on the south slope of the Mt. Everest region. All of the variables analyzed showed a continuing deglaciation trend. The phenomenon appears to be accelerated in recent decades, particularly with regards to the shrinkage of surface area and the upward shift of the SLA. Based on this evidence, we decided to deepen the analysis to shed light on what may be the boundary conditions favoring the process and the possible drivers of change. Many authors (Salerno et al., 2008; Bolch et al., 2010; Yao et al., 2012; Schmidt and Nüsser, 2012) have already shown that the glacier shrinkage rate is related to the size of the glacier. Therefore, we divided the glaciers into three-dimensional classes (< 2.5 km²; 2.5–10 km²; > 10 km²) that were defined to contain a similar number of glaciers in each class. For each variable, we analyzed the differences in cumulative changes in the overall period (1962–2011) (Fig. 6a, c, e) and the differences in the annual rate of change between two periods (1962–1992 and 1992–2011) (Fig. 6b, d, f).

In Fig. 6a, we observe that the cumulative terminus retreat, in the overall 1962–2011 period, is 55 m (median) for glaciers < 2.5 km² and 433 m (median) for glaciers > 10 km². If we compared these values with the length of the ablation area of the glacier we would get a percentage of terminus retreat double for the largest glaciers (2.3 %, 4.3 %, respectively). We have already discussed that these glaciers, regardless of size, did not show a significant increase in the annual retreat rate. In Fig. 6b, we note that the annual retreat rate is increasing for all classes and especially for the glaciers of greater size, but these differences are not significant even considering the glaciers

Tracing glacier changes since the 1960s

S. Thakuri et al.

Title Page

Abstract

Introduction

Conclusions

References

Tables

Figures



Back

Close

Full Screen / Esc

Printer-friendly Version

Interactive Discussion



size ($p = 0.41$, $p = 0.52$, $p = 0.13$), which means that each class contains a significant number of glaciers that are not currently accelerating the process.

Regarding the glacier surface area losses, we showed a general decrease of $13.0 \pm 3.1\%$. In Fig. 6c, we can observe that the percentage of shrinkage is $9 \pm 3.3\%$ for the glaciers $> 10 \text{ km}^2$, but that this percentage rises to $36 \pm 4.8\%$ for the glaciers $< 2.5 \text{ km}^2$. For the glaciers $< 1 \text{ km}^2$, this percentage rises to $42 \pm 5.8\%$. Comparing the annual rate of shrinkage, we note an interesting change (Fig. 6d): the rate is increasing in the 1992–2011 period from the previous period for all classes, but it is especially increasing for glaciers of larger size. By testing the significance of these differences, only the rate of glaciers $> 10 \text{ km}^2$ were significant between two periods. The p values were 0.13, 0.80, and 0.03, respectively, compared to the overall significant shrinkage, as highlighted above.

A similar picture emerges if we consider the changes in the SLA (Fig. 6f). Significant differences were found between two periods only for glaciers $> 10 \text{ km}^2$ ($p = 0.15$, $p = 0.25$, $p = 0.03$) compared to a significant overall shift in SLA, as highlighted above. It is also interesting to note (Fig. 6e) that these glaciers presented median upward shifts equal to more than 220 m, while smaller glaciers showed increases of approximately half.

Based on this evidence, we can say that from the 1960s to today, the glaciers that have undergone the most climate impact are small ones, but it is also true that over the last two decades, the condition of larger glaciers has worsened much more. To find the reasons for this differential acceleration, we remember that, as set out by Salerno et al. (2008), the largest glaciers are south oriented and located at higher altitudes. In the present study, we confirm these statements using the glacier outlines of 2011 traced on satellite imagery and with a DEM with a higher resolution ($r = 0.62$, $p < 0.05$ for the relationship size/aspect, $r = 0.57$, $p < 0.05$ for the relationship size/mean glacier elevation). Furthermore, Salerno et al. (2008) observed that in the 1960–1990 period, larger glaciers decreased less in size and that some of them were on the rise. This divergent behavior was explained by considering the increase of

Tracing glacier changes since the 1960s

S. Thakuri et al.

Title Page

Abstract

Introduction

Conclusions

References

Tables

Figures

◀

▶

◀

▶

Back

Close

Full Screen / Esc

Printer-friendly Version

Interactive Discussion



Tracing glacier changes since the 1960s

S. Thakuri et al.

Title Page

Abstract

Introduction

Conclusions

References

Tables

Figures

◀

▶

◀

▶

Back

Close

Full Screen / Esc

Printer-friendly Version

Interactive Discussion



dian upward shifts equal to more than 220 m, while the smaller ones have increases of about half of that. Temperature variations, despite being the primary cause eliciting glacier response, cannot alone account for why these glaciers, located at higher altitudes, reordered such a high upward shift of SLA and why their shrinkage annual rate increased much more than that of the other glaciers. We propose that in the case of larger glaciers that have accelerated shrinkage processes, the effects of the current weakening of the Asian monsoon were added to the effects of increasing temperatures because the glaciers' orientation is aligned with the prevailing precipitation, which makes these glaciers more sensitive to variations in precipitation than to variations in temperatures.

We noted that the shrinkage of these glaciers is lower than in the entire Himalayan range. Their higher elevations have reduced the warming impact, but have not been able to exclude these glaciers from a relentlessly continuous and slow recession process over the past fifty years.

It should be noted that the majority of studies on glacier area changes, as noted by Hewitt (2007), suffer from the absence of high-altitude data, which makes it problematic to extrapolate the changes observed at weather stations to the glaciers. In the near future, a study is planned to explore the small-scale climate variability of the south slope of Mt. Everest by analyzing the temperature and precipitation time series reconstructed from weather stations located at the “Pyramid” meteorological observatory, which can be used to support the cause of the recent observed changes.

Furthermore, we have planned a study, complementary to present work, which will include all of the lakes in the region. Our aim is to more clearly determine the magnitude of the changes affecting water resources on the south slopes of Mt. Everest region during the second half of the 20th century.

Supplementary material related to this article is available online at <http://www.the-cryosphere-discuss.net/7/5389/2013/tcd-7-5389-2013-supplement.pdf>.

Acknowledgements. This work was supported by the MIUR through Ev-K2-CNR/SHARE and CNR-DTA/NEXTDATA projects within the framework of the Ev-K2-CNR and Nepal Academy of Science and Technology (NAST) collaboration in Nepal. S. Thakuri is recipient of the Intergovernmental Panel on Climate Change (IPCC) Scholarship Award under the collaboration between the IPCC Scholarship Programme and the Prince Albert II of Monaco Foundation's Young Researchers Scholarships Initiative. T. Bolch acknowledges funding through Deutsche Forschungsgemeinschaft (DFG).

References

- Ageta, Y. and Fujita, K.: Characteristics of mass balance of summer-accumulation type glaciers in the Himalayas and Tibetan Plateau, *Z. Gletscherkd. Glazialgeol.*, 32, 61–65, 1996.
- Asahi, K.: Equilibrium-line altitudes of the present and Last Glacial Maximum in the eastern Nepal Himalayas and their implications for SW monsoon climate, *Quatern. Int.*, 212, 26–34, 2010.
- Bagla, P.: No sign yet of Himalayan meltdown, Indian report finds, *Science*, 326, 924–925, 2009.
- Benn, D. I., Bolch, T., Hands, K., Gulley, J., Luckman, A., Nicholson, L. I., Quincey, D., Thompson, S., Toumi, R., and Wiseman, S.: Response of debris-covered glaciers in the Mount Everest region to recent warming, and implications for outburst flood hazards, *Earth-Sci. Rev.*, 114, 156–174, 2012.
- Bhambri, R., Bolch, T., Chaujar, R. K., and Kulshreshtha, S. C.: Glacier changes in the Garhwal Himalaya, India, from 1968 to 2006 based on remote sensing, *J. Glaciol.*, 57, 543–556, 2011.
- Bhambri, R., Bolch, T., Chaujar, R. K.: Frontal recession of Gangotri glacier, Garhwal Himalayas, from 1965 to 2006, measured through high-resolution remote sensing data, *Curr. Sci.*, 102, 489–494, 2012.
- Bolch, T., Buchroithner, M., Pieczonka, T., and Kunert, A.: Planimetric and volumetric glacier changes in the Khumbu Himalaya since 1962 using Corona, Landsat TM and ASTER data, *J. Glaciol.*, 54, 592–600, 2008a.
- Bolch, T., Buchroithner, M. F., Peters, J., Baessler, M., and Bajracharya, S.: Identification of glacier motion and potentially dangerous glacial lakes in the Mt. Everest region/Nepal using

Tracing glacier changes since the 1960s

S. Thakuri et al.

Title Page

Abstract

Introduction

Conclusions

References

Tables

Figures

◀

▶

◀

▶

Back

Close

Full Screen / Esc

Printer-friendly Version

Interactive Discussion



Tracing glacier changes since the 1960s

S. Thakuri et al.

Title Page

Abstract

Introduction

Conclusions

References

Tables

Figures

◀

▶

◀

▶

Back

Close

Full Screen / Esc

Printer-friendly Version

Interactive Discussion



spaceborne imagery, *Nat. Hazards Earth Syst. Sci.*, 8, 1329–1340, doi:10.5194/nhess-8-1329-2008, 2008b.

Bolch, T., Yao, T., Kang, S., Buchroithner, M. F., Scherer, D., Maussion, F., Huintjes, E., and Schneider, C.: A glacier inventory for the western Nyainqentanglha Range and the Nam Co Basin, Tibet, and glacier changes 1976–2009, *The Cryosphere*, 4, 419–433, doi:10.5194/tc-4-419-2010, 2010.

Bolch, T., Pieczonka, T., and Benn, D. I.: Multi-decadal mass loss of glaciers in the Everest area (Nepal Himalaya) derived from stereo imagery, *The Cryosphere*, 5, 349–358, doi:10.5194/tc-5-349-2011, 2011.

10 Bolch, T., Kulkarni, A., Kääb, A., Huggel, C., Paul, F., Cogley, J. G., Frey, H., Kargel, J. S., Fujita, K., Scheel, M., Bajracharya, S., and Stoffel, M.: The state and fate of Himalayan glaciers, *Science*, 336, 310–314, 2012.

Chen, J., Zhu, X., Vogelmann, J. E., Gao, F., and Jin, S.: A simple and effective method for filling gaps in Landsat ETM+ SLC-off images, *Remote Sens. Environ.*, 115, 1053–1064, 2011.

15 Chinn, T. J., Heydenrych, C., and Salinger, M. J.: Use of the ELA as a practical method of monitoring glacier response to climate in New Zealand's Southern Alps, *J. Glaciol.*, 51, 85–95, 2005.

Cogley, J. G., Kargel, J. S., Kaser, G., and Van der Veen, C. J.: Tracking the source of glacier misinformation, *Science*, 327, p. 522, 2010.

20 Cook, E. R., Krusic, P. J., and Jones, P. D.: Dendroclimatic signals in long tree-ring chronologies from the Himalayas of Nepal, *Int. J. Climatol.*, 23, 707–732, 2003.

Diodato, N., Bellocchi, G., and Tartari, G.: How do Himalayan areas respond to global warming?, *Int. J. Climatol.*, 32, 975–982, 2012.

25 Fowler, H. J. and Archer, D. R.: Conflicting signals of climatic change in the upper Indus Basin, *J. Climate*, 19, 4276–4293, 2006.

Frey, H., Paul, F., and Strozzi, T.: Compilation of a glacier inventory for the western Himalayas from satellite data: methods, challenges and results, *Remote Sens. Environ.*, 124, 832–843, 2012.

30 Fujita, K. and Nuimura, T.: Spatially heterogeneous wastage of Himalayan glaciers, *Proc. Natl. Acad. Sci. USA*, 108, 14011–14014, 2011.

Fujita, K., Thompson, L. G., Ageta, Y., Yasunari, T., Kajikawa, Y., Sakai, A., and Takeuchi, N.: Thirty-year history of glacier melting in the Nepal Himalayas, *J. Geophys. Res.*, 111, D03109, doi:10.1029/2005JD005894, 2006.

Tracing glacier changes since the 1960s

S. Thakuri et al.

Title Page

Abstract

Introduction

Conclusions

References

Tables

Figures

◀

▶

◀

▶

Back

Close

Full Screen / Esc

Printer-friendly Version

Interactive Discussion



Gardelle, J., Arnaud, Y., and Berthier, E.: Contrasted evolution of glacial lakes along the Hindu Kush Himalaya mountain range between 1990 and 2009, *Global Planet. Change*, 75, 47–55, 2011.

Gardelle, J., Berthier, E., Arnaud, Y., and Käab, A.: Region-wide glacier mass balances over the Pamir-Karakoram-Himalaya during 1999–2011, *The Cryosphere*, 7, 1263–1286, doi:10.5194/tc-7-1263-2013, 2013.

Grosse, G., Schirmer, L., Kunitsky, V. V., and Hubberten, H. W.: The use of CORONA images in remote sensing of periglacial geomorphology: an illustration from the NE Siberian coast, *Permafrost Periglac.*, 16, 163–172, 2005.

Hall, D. K., Bayr, K. J., Schoner, W., Bindschadler, R. A., and Chien, J. Y. L.: Consideration of the errors inherent in mapping historical glacier positions in Austria from the ground and space (1893–2001), *Remote Sens. Environ.*, 86, 566–577, 2003.

Hess, H.: *Die Gletscher*, Braunschweig, 406 pp., 1904.

Hewitt, K.: Tributary glacier surges: an exceptional concentration at Panmah Glacier, Karakoram Himalaya, *J. Glaciol.*, 53, 181–188, 2007.

Hoelzle, M., Chinn, T., Stumm, D., Paul, F., Zemp, M., and Haeberli, W.: The application of inventory data for estimating past climate change effects on mountain glaciers: a comparison between the European Alps and the Southern Alps of New Zealand, *Global Planet. Change*, 56, 69–82, 2007.

Hooke, R. L.: *Principles of Glacier Mechanics*, Cambridge University Press, 429 pp., 2005.

Ichayanagi, K., Yamanaka, M. D., Muraji, Y., and Vaidya, B. K.: Precipitation in Nepal between 1987 and 1996, *Int. J. Climatol.*, 27, 1753–1762, 2007.

Jhajharia, D. and Singh, V. P.: Trends in temperature, diurnal temperature range and sunshine duration in Northeast India, *Int. J. Climatol.*, 31, 1353–1367, 2011.

Jin, R., Li, X., Che, T., Wu, L., and Mool, P.: Glacier area changes in the Pumqu river basin, Tibetan Plateau, between the 1970s and 2001, *J. Glaciol.*, 51, 607–610, 2005.

Jones, P. D. and Moberg, A.: Hemispheric and large-scale surface air temperature variations: an extensive revision and an update to 2001, *J. Climate*, 16, 206–223, 2003.

Käab, A., Berthier, E., Nuth, C., Gardelle, J., and Arnaud, Y.: Contrasting patterns of early twenty-first-century glacier mass change in the Himalayas, *Nature*, 488, 495–498, 2012.

Karma, Ageta, Y., Naito, N., Iwata, S., and Yabuki, H.: Glacier distribution in the Himalayas and glacier shrinkage from 1963 to 1993 in the Bhutan Himalayas, *Bull. Glaciol. Res.*, 20, 29–40, 2003.

Tracing glacier changes since the 1960s

S. Thakuri et al.

Title Page

Abstract

Introduction

Conclusions

References

Tables

Figures

◀

▶

◀

▶

Back

Close

Full Screen / Esc

Printer-friendly Version

Interactive Discussion



- Karpilo, R. D. J.: Glacier monitoring techniques, in: Geological Monitoring, edited by: Young, R. and Norby, L., The Geological Society of America, Boulder, Colorado, 141–162, 2009.
- Kattel, D. B. and Yao, T.: Recent temperature trends at mountain stations on the southern slope of the Central Himalayas, *J. Earth Syst. Sci.*, 122, 215–227, 2013.
- 5 Kaufman, Y. J., Koren, I., Remer, L. A., Tanre, D., Ginoux, P., and Fan, S.: Dust transport and deposition observed from the Terra-moderate Resolution Imaging Spectroradiometer (MODIS) spacecraft over the Atlantic Ocean, *J. Geophys. Res.-Atmos.*, 110, D10S12, doi:10.1029/2003JD004436, 2005.
- Kayastha, R. B. and Harrison, S. P.: Changes of the equilibrium-line altitude since the little ice age in the Nepalese Himalaya, *Ann. Glaciol.*, 48, 93–99, 2008.
- 10 Kerschner, H.: Statistical modelling of equilibrium-line altitudes of Hintereisferner, central Alps, Austria, 1859-present, *Ann. Glaciol.*, 24, 111–115, 1997.
- Koblet, T., Gärtner-Roer, I., Zemp, M., Jansson, P., Thee, P., Haeberli, W., and Holmlund, P.: Re-analysis of multi-temporal aerial images of Storglaciären, Sweden (1959–99) – Part 1: Determination of length, area, and volume changes, *The Cryosphere*, 4, 333–343, doi:10.5194/tc-4-333-2010, 2010.
- 15 Kresse, W. and Danko, D. M.: Springer Handbook of Geographic Information, Springer Verlag, 1120 pp., 2011.
- Kuhn, M.: Climate and glaciers. Sea level, ice and climatic change, in: Proceedings of the Canberra Symposium, edited by: Allison, I., December 1979, IASH Publ. 131, 3–20, 1981.
- Kulkarni, A. V., Rathore, B. P., Singh, S. K., and Bahuguna, I. M.: Understanding changes in the Himalayan cryosphere using remote sensing techniques, *Int. J. Remote Sens.*, 32, 601–615, 2011.
- 20 Lami, A., Marchetto, A., Musazzi, S., Salerno, F., Tartari, G., Guilizzoni, P., Rogora, M., and Tartari, G. A.: Chemical and biological response of two small lakes in the Khumbu Valley, Himalayas (Nepal) to short-term variability and climatic change as detected by long-term monitoring and paleolimnological methods, *Hydrobiologia*, 648, 189–205, 2010.
- Leonard, K. C. and Fountain, A. G.: Map-based methods for estimating glacier equilibrium-line altitudes, *J. Glaciol.*, 49, 329–336, 2003.
- 30 Liu, X. and Chen, B.: Climatic warming in the Tibetan Plateau during recent decades, *Int. J. Climatol.*, 20, 1729–1742, 2000.
- Lorenz, H.: Integration of Corona and Landsat Thematic Mapper data for bedrock geological studies in the high Arctic, *Int. J. Remote Sens.*, 25, 5143–5162, 2004.

Tracing glacier changes since the 1960s

S. Thakuri et al.

Title Page

Abstract

Introduction

Conclusions

References

Tables

Figures

◀

▶

◀

▶

Back

Close

Full Screen / Esc

Printer-friendly Version

Interactive Discussion



McFadden, E. M., Ramage, J., and Rodbell, D. T.: Landsat TM and ETM+ derived snowline altitudes in the Cordillera Huayhuash and Cordillera Raura, Peru, 1986–2005, *The Cryosphere*, 5, 419–430, doi:10.5194/tc-5-419-2011, 2011.

Mehta, M., Dobhal, D. P., and Bisht, M. P. S.: Change of Tipra Glacier in the Garhwal Himalaya, India, between 1962 and 2008, *Prog. Phys. Geogr.*, 35, 721–738, 2011.

Mool, P. K., Bajracharya, S. R., and Joshi, S. P.: Inventory of Glaciers, Glacial Lakes and Glacial Lake Outburst Floods, Monitoring and Early Warning Systems in the Hindu Kush-Himalaya Region, ICIMOD, Nepal, 2001.

Müller, F.: Present and Late Pleistocene Equilibrium Line Altitudes in the Mt. Everest Region – An Application of the Glacier Inventory, IAHS-AISH Publication, 126, 75–94, 1980.

Naidu, C. V., Durgalakshmi, K., Muni Krishna, K., Ramalingeswara, S., Satyanarayan, G. C., Lakshminarayana, P., and Rao, L. M.: Is summer monsoon rainfall decreasing over India in the global warming era?, *J. Geophys. Res.-Atmos.*, 114, D24108, doi:10.1029/2008JD011288, 2009.

Nakawo, M., Yabuki, H., and Sakai, A.: Characteristics of Khumbu Glacier, Nepal Himalaya: recent change in the debris-covered area, *Ann. Glaciol.*, 28, 118–122, 1999.

Nie, Y., Zhang, Y., Liu, L., and Zhang, J.: Glacial change in the vicinity of Mt. Qomolangma (Everest), central high Himalayas since 1976, *J. Geogr. Sci.*, 20, 667–686, 2010.

Numura, T., Fujita, K., Yamaguchi, S., and Sharma, R. R.: Elevation changes of glaciers revealed by multitemporal digital elevation models calibrated by GPS survey in the Khumbu region, Nepal Himalaya, 1992–2008, *J. Glaciol.*, 58, 648–656, 2012.

Ouimet, W., Whipple, K., and Granger, D.: Beyond threshold hillslopes: channel adjustment to base-level fall in tectonically active mountain ranges, *Geology*, 37, 579–582, 2009.

Owen, L. A. and Benn, D. I.: Equilibrium-line altitudes of the Last Glacial Maximum for the Himalaya and Tibet: an assessment and evaluation of results, *Quatern. Int.*, 138–139, 55–78, 2005.

Pal, I. and Al-Tabbaa, A.: Regional changes in extreme monsoon rainfall deficit and excess in India, *Dynam. Atmos. Oceans*, 49, 206–214, 2010.

Palazzi, E., von Hardenberg, J., and Provenzale, A.: Precipitation in the Hindu-Kush Karakoram Himalaya: observations and future scenarios, *J. Geophys. Res.-Atmos.*, 118, 85–100, 2013.

Parkinson, C. L., Ward, A., and King, M. D.: Earth Science Reference Handbook, a Guide to NASA's Earth Science Program and Earth Observing Satellite Missions, National Aeronautics and Space Administration, 2006.

Tracing glacier changes since the 1960s

S. Thakuri et al.

Title Page

Abstract

Introduction

Conclusions

References

Tables

Figures

◀

▶

◀

▶

Back

Close

Full Screen / Esc

Printer-friendly Version

Interactive Discussion



- Paul, F., Kaab, A., Maisch, M., Kellenberger, T., and Haeberli, W.: The new remote-sensing-derived Swiss glacier inventory: methods, *Ann. Glaciol.*, 34, 355–361, 2002.
- Paul, F., Huggel, C., and Kääb, A.: Combining satellite multispectral image data and a digital elevation model for mapping debris-covered glaciers, *Remote Sens. Environ.*, 89, 510–518, 2004.
- Paul, F., Barry, R. G., Cogley, J. G., Frey, H., Haeberli, W., Ohmura, A., Ommanney, C. S. L., Raup, B., Rivera, A., and Zemp, M.: Recommendations for the compilation of glacier inventory data from digital sources, *Ann. Glaciol.*, 50, 119–126, 2009.
- Pelto, M.: Utility of late summer transient snowline migration rate on Taku Glacier, Alaska, *The Cryosphere*, 5, 1127–1133, doi:10.5194/tc-5-1127-2011, 2011.
- Pieczonka, T., Bolch, T., Wei, J., and Liu, S.: Heterogeneous mass loss of glaciers in the Aksu-Tarim Catchment (Central Tien Shan) revealed by 1976 KH-9 Hexagon and 2009 SPOT-5 stereo imagery, *Remote Sens. Environ.*, 130, 233–244, 2013.
- Quincey, D. J., Luckman, A., and Benn, D.: Quantification of Everest region glacier velocities between 1992 and 2002, using satellite radar interferometry and feature tracking, *J. Glaciol.*, 55, 596–606, 2009.
- Rabatel, A., Dedieu, J. P., and Vincent, C.: Using remote-sensing data to determine equilibrium-line altitude and mass-balance time series: validation on three French glaciers, 1994–2002, *J. Glaciol.*, 51, 539–546, 2005.
- Rabatel, A., Bermejo, A., Loarte, E., Soruco, A., Gomez, J., Leonardini, G., Vincent, C., and Sicart, J. E.: Can the snowline be used as an indicator of the equilibrium line and mass balance for glaciers in the outer tropics?, *J. Glaciol.*, 58, 1027–1036, 2012.
- Racoviteanu, A., Williams, M., and Barry, R.: Optical remote sensing of glacier characteristics: a review with focus on the Himalaya, *Sensors*, 8, 3355–3383, 2008.
- Raina, V. K.: Himalayan Glaciers: a State-of-Art Review of Glacial Studies, Glacier Retreat and Climate Change, MoEF Discussion Paper, Government of India – Ministry of Environment and Forests, 56 pp., 2009.
- Ramanathan, V., Chung, C., Kim, D., Bettge, T., Buja, L., Kiehl, J. T., Washington, W. M., Fu, Q., Sikka, D. R., and Wild, M.: Atmospheric brown clouds: impacts on south Asian climate and hydrological cycle, *Proc. Natl. Acad. Sci. USA*, 102, 5326–5333, 2005.
- Rao, Y. P.: Southwest Monsoon, India Meteorological Department, Meteorological Monograph, New Delhi, 366 pp., 1976.

Tracing glacier changes since the 1960s

S. Thakuri et al.

Title Page

Abstract

Introduction

Conclusions

References

Tables

Figures

◀

▶

◀

▶

Back

Close

Full Screen / Esc

Printer-friendly Version

Interactive Discussion



- Ren, J., Jing, Z., Pu, J., and Qin, X.: Glacier variations and climate change in the central Himalaya over the past few decades, *Ann. Glaciol.*, 43, 218–222, 2006.
- Rodriguez-Galiano, V. F., Pardo-Iguzquiza, E., Chica-Olmo, M., Mateos, J., Rigol-Sanchez, J. P., and Vega, M.: A comparative assessment of different methods for Landsat 7/ETM+ pan-sharpening, *Int. J. Remote Sens.*, 33, 6574–6599, 2012.
- Rosenholm, D. and Akerman, D.: Digital orthophotos from IRS – production and utilization, in: IAPRS, edited by: Fritsch, D., Englich, M., and Sester, M., ISPRS Commission IV Symposium on GIS – Between Visions and Applications, Stuttgart, Germany, 32, 501–505, 1998.
- Salerno, F., Buraschi, E., Bruccoleri, G., Tartari, G., and Smiraglia, C.: Glacier surface-area changes in Sagarmatha National Park, Nepal, in the second half of the 20th century, by comparison of historical maps, *J. Glaciol.*, 54, 738–752, 2008.
- Salerno, F., Viviano, G., Thakuri, S., Flury, B., Maskey, R. K., Khanal, S. N., Bhujju, D., Carrer, M., Bhochohibhoya, S., Melis, M. T., Giannino, F., Staiano, A., Carteni, F., Mazzoleni, S., Cogo, A., Sapkota, A., Shrestha, S., Pandey, R. K., and Manfredi, E. C.: Energy, forest, and indoor air pollution models for Sagarmatha National Park and Buffer zone, Nepal: implementation of a participatory modeling framework, *Mt. Res. Dev.*, 30, 113–126, 2010a.
- Salerno, F., Cuccillato, E., Caroli, P., Bajracharya, B., Manfredi, E. C., Viviano, G., Thakuri, S., Flury, B., Basani, M., Giannino, F., and Panzeri, D.: Experience with a hard and soft participatory modeling framework for social ecological system management in Mount Everest (Nepal) and K2 (Pakistan) protected areas, *Mt. Res. Dev.*, 30, 80–93, 2010b.
- Salerno, F., Thakuri, S., D’Agata, C., Smiraglia, C., Manfredi, E. C., Viviano, G., and Tartari, G.: Glacial lake distribution in the Mount Everest region: Uncertainty of measurement and conditions of formation, *Global Planet. Change*, (92–93), 30–39, 2012.
- Salerno, F., Viviano, G., Mangredi, E. C., Caroli, P., Thakuri, S., and Tartari, G.: Multiple Carrying Capacities from a management-oriented perspective to operationalize sustainable tourism in protected area, *J. Environ. Manag.*, 128, 116–125, 2013.
- Sano, M., Furuta, F., Kobayashi, O., and Sweda, T.: Temperature variations since the mid-18th century for western Nepal, as reconstructed from tree-ring width and density of *Abies spectabilis*, *Dendrochronologia*, 23, 83–92, 2005.
- Scherler, D., Bookhagen, B., and Strecker, M. R.: Spatially variable response of Himalayan glaciers to climate change affected by debris cover, *Nat. Geosci.*, 4, 156–159, 2011.

Tracing glacier changes since the 1960s

S. Thakuri et al.

Title Page

Abstract

Introduction

Conclusions

References

Tables

Figures

◀

▶

◀

▶

Back

Close

Full Screen / Esc

Printer-friendly Version

Interactive Discussion



Schmidt, S. and Nüsser, M.: Changes of high altitude glaciers from 1969 to 2010 in the trans-Himalayan Kang Yatze Massif, Ladakh, Northwest India, *Arct. Antarct. Alp. Res.*, 44, 107–121, 2012.

Schneider, E.: Begleitworte zur Karte Khumbu Himal und zur Namensgebung, in: *Khumbu Himal*, edited by Hellmich, W., Universitasverlag Wagner, Innsbruck, 430–446, 1967.

Shapiro, S. S. and Wilk, M. B.: An analysis of variance test for normality (complete samples), *Biometrika*, 52, 591–611, 1965.

Sharma, K. P., Moore, B., and Vorosmarty, C. J.: Anthropogenic, climatic, and hydrologic trends in the Kosi basin, Himalaya, *Clim. Change*, 47, 141–165, 2000.

Streets, D. G., Yan, F., Chin, M., Diehl, T., Mahowald, N., Schultz, M., Wild, M., Wu, Y., and Yu, C.: Anthropogenic and natural contributions to regional trends in aerosol optical depth, 1980–2006, *J. Geophys. Res.-Atmos.*, 114, D00D18, doi:10.1029/2008JD011624, 2009.

Tartari, G., Verza, G., and Bertolami, L.: Meteorological data at the Pyramid Observatory Laboratory (Khumbu Valley, Sagarmatha National Park, Nepal), in: *Limnology of High Altitude Lakes in the Mt. Everest Region (Nepal)*, edited by: Lami, A. and Giussani, G., *Mem. Ist. Ital. Idrobiol.*, 57, 23–40, 2002.

Tartari, G., Salerno, F., Buraschi, E., Bruccoleri, G., and Smiraglia, C.: Lake surface area variations in the North-Eastern sector of Sagarmatha National Park (Nepal) at the end of the 20th Century by comparison of historical maps, *J. Limnol.*, 67, 139–154, 2008.

Tennant, C., Menounos, B., Ainslie, B., Shea, J., and Jackson, P.: Comparison of modeled and geodetically-derived glacier mass balance for Tiedemann and Klinaklini glaciers, southern Coast Mountains, British Columbia, Canada, *Global Planet. Change*, 82–83, 74–85, 2012.

Thompson, L. G., Thompson, E. M., Brecher, H., Davis, M., Leon, B., Les, D., Lin, P. N., Mashiotta, T., and Mountain, K.: Abrupt tropical climate change: past and present, *Proc. Natl. Acad. Sci. USA*, 103, 10536–10543, 2006.

Ueno, K., Toyotsu, K., Bertolani, L., and Tartari, G.: Stepwise onset of monsoon weather observed in the Nepal Himalayas, *Mon. Weather Rev.*, 132, 2507–2522, 2008.

Walford, N.: *Practical Statistics for Geographers and Earth Scientists*, John Wiley and Sons, 440 pp., 2011.

Wang, W., Yao, T., and Yang, X.: Variations of glacial lakes and glaciers in the Boshula mountain range, southeast Tibet, from the 1970s to 2009, *Ann. Glaciol.*, 52, 9–17, 2011.

Wild, M.: The heat balance of the Earth in GCM simulations of present and future climate, *Zuercher Geografische Schriften No. 68*, Verlag der Fachvereine, Zuerich, 188 pp., 1997.

Tracing glacier changes since the 1960s

S. Thakuri et al.

Title Page

Abstract

Introduction

Conclusions

References

Tables

Figures

◀

▶

◀

▶

Back

Close

Full Screen / Esc

Printer-friendly Version

Interactive Discussion



- Wild, M.: Global dimming and brightening: a review, *J. Geophys. Res.-Atmos.*, 114, D00D16, doi:10.1029/2008JD011470, 2009.
- Wild, M., Gilgen, H., Roesch, A., Ohmura, A., Long, C. N., Dutton, E. G., Forgan, B., Kallis, A., Russak, V., and Tsvetkov, A.: From dimming to brightening: decadal changes in solar radiation at Earth's surface, *Science*, 308, 847–850, 2005.
- Wu, B.: Weakening of Indian summer monsoon in recent decades, *Adv. Atmos. Sci.*, 22, 21–29, 2005.
- Yamada, T.: Glacier lake and its outburst flood in the Nepal Himalaya, Tokyo, Japanese Society of Snow and Ice, Data Center for Glacier Research (Monograph 1), 1998.
- Yamada, T., Shiraiwa, T., Iida, H., Kadota, T., Watanabe, T., Rana, B., Ageta, Y., and Fushimi, H.: Fluctuations of the glaciers from the 1970s to 1989 in the Khumbu, Shorong and Langtang regions, Nepal Himalayas, *Bull. Glacier Res.*, 10, 11–19, 1992.
- Yao, T., Thompson, L., Yang, W., Yu, W., Gao, Y., Guo, X., Yang, X., Duan, K., Zhao, H., Xu, B., Pu, J., Lu, A., Xiang, Y., Kattel, D. B., and Joswiak, D.: Different glacier status with atmospheric circulations in Tibetan Plateau and surroundings, *Nat. Clim. Change*, 2, 663–667, 2012.
- Ye, Q., Kang, S., Chen, F., and Wang, J.: Monitoring glacier variations on Geladandong mountain, central Tibetan Plateau, from 1969 to 2002 using remote-sensing and GIS technologies, *J. Glaciol.*, 52, 537–545, 2006.
- Ye, Q., Zhong, Z., Kang, S., Stein, A., Wei, Q., and Liu, J.: Monitoring glacier and supra-glacier lakes from space in Mt. Qomolangma region of the Himalayas on the Tibetan Plateau in China, *J. Mt. Sci. [China]*, 6, 211–220, 2009.

Tracing glacier changes since the 1960s

S. Thakuri et al.

Title Page

Abstract

Introduction

Conclusions

References

Tables

Figures

◀

▶

◀

▶

Back

Close

Full Screen / Esc

Printer-friendly Version

Interactive Discussion



Table 1. Data sources used in this study.

Abbreviation used in the text	Satellite image	Acquisition date	Spatial resolution (m)	Sensor	Scene ID
Corona-62	Corona	15 Dec 1962	~ 8	KH-4	DS009050054DF172_172 DS009050054DA174_174 DS009050054DA175_175
Corona-70	Corona	20 Nov 1970	~ 5	KH-4B	DS1112-1023DA163_163 DS1112-1023DF157_157 LM21510411975306AAA05
Landsat-75	Landsat 4	2 Nov 1975	60	MSS	
Landsat-92	Landsat 5	17 Nov 1992	30	TM	ETP140R41_5T19921117
Landsat-00	Landsat 7	30 Oct 2000	15 ^a	ETM+	LE71400412000304SGS00 ALAV2A146473040
ALOS-08	ALOS	24 Oct 2008	10	AVNIR-2 ETM+	
Landsat-11	Landsat 7	30 Nov 2011	15 ^{a,b}		LE71400412011334EDC00
Abbreviation used in the text	Topographic map	Acquisition date	Scale	Acquisition technique	
KHmap-50s	Khumbu Himal map (Schneider Map)	late 1950s	1 : 50 000	Photographic survey in 1921, terrestrial photogrammetric survey of 1935 and 1939 (Schneider, 1967)	
TISmap-63	Topographic map of Indian survey	1963	1 : 50 000	Vertical aerial photographic survey 1957–1959 and field survey in 1963 (Yamada, 1998)	
OTNmap-92	Official topographic map of Nepal	1992	1 : 50 000	Aerial photogrammetry (1992) and field survey (1996), published in 1997 by Government of Nepal	

^a Pan-sharpened images; ^b SLC-off image.

Tracing glacier changes since the 1960s

S. Thakuri et al.

Table 2. Glacier changes from 1962 to 2011 in the Mt. Everest region.

Period	Terminus position change (Δ Term)		Surface area change (Δ Surf)		Snow-line altitude change (Δ SLA)		Debris coverage change (Δ DebrisCov)	
	Cumulative length (m)	Median annual rate (m a^{-1})	Cumulative area (%)	Median annual rate ($\% \text{ a}^{-1}$)	Cumulative altitude (m)	Median annual rate (m a^{-1})	Cumulative area (%)	Median annual rate ($\% \text{ a}^{-1}$)
1962–1975	-116 ± 30	-6.0 ± 2.3	-1.7 ± 9.7	-0.27 ± 0.75	26 ± 30	1.3 ± 2.3	3.8 ± 10.6	0.13 ± 0.84
1975–1992	-208 ± 11	-2.6 ± 1.9	-4.8 ± 4.1	-0.29 ± 0.65	66 ± 11	2.6 ± 1.9	5.7 ± 4.2	0.27 ± 0.67
1992–2000	-285 ± 9	-7.0 ± 1.6	-7.7 ± 3.0	-0.41 ± 0.60	94 ± 9	2.3 ± 1.6	8.8 ± 3.8	0.27 ± 0.72
2000–2008	-367 ± 6	-5.8 ± 1.1	-11.3 ± 2.3	-0.63 ± 0.38	151 ± 6	6.9 ± 1.1	15.8 ± 2.1	0.89 ± 0.55
2008–2011	-403 ± 9	-3.0 ± 3.0	-13.0 ± 3.1	-0.76 ± 0.99	182 ± 9	8.7 ± 3.0	17.6 ± 2.8	0.46 ± 1.18
1962–2011	-403 ± 9	6.1 ± 0.2	-13.0 ± 3.1	0.42 ± 0.06	182 ± 9	3.9 ± 0.17	17.6 ± 2.8	0.21 ± 0.07

[Title Page](#)
[Abstract](#)
[Introduction](#)
[Conclusions](#)
[References](#)
[Tables](#)
[Figures](#)
[Back](#)
[Close](#)
[Full Screen / Esc](#)
[Printer-friendly Version](#)
[Interactive Discussion](#)


Tracing glacier changes since the 1960s

S. Thakuri et al.

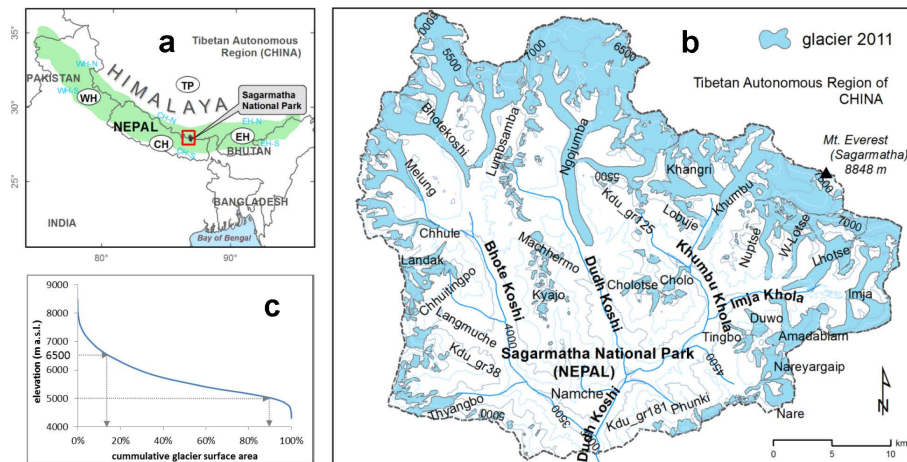


Fig. 1. (a) Location of the study area: the Sagarmatha National Park (SNP), where the abbreviations CH, WH, EH, and TP represent Central Himalaya, Western Himalaya, Eastern Himalaya and Tibetan Plateau, respectively (suffixes -N and -S indicate the northern and southern slopes). (b) Focused map of the SNP in 2011 showing the distribution of 29 glaciers considered in this study with a surface area $> 1 \text{ km}^2$. (c) The hypsometric curve of the glaciers in 2011.

Title Page

Abstract

Introduction

Conclusions

References

Tables

Figures

◀

▶

◀

▶

Back

Close

Full Screen / Esc

Printer-friendly Version

Interactive Discussion



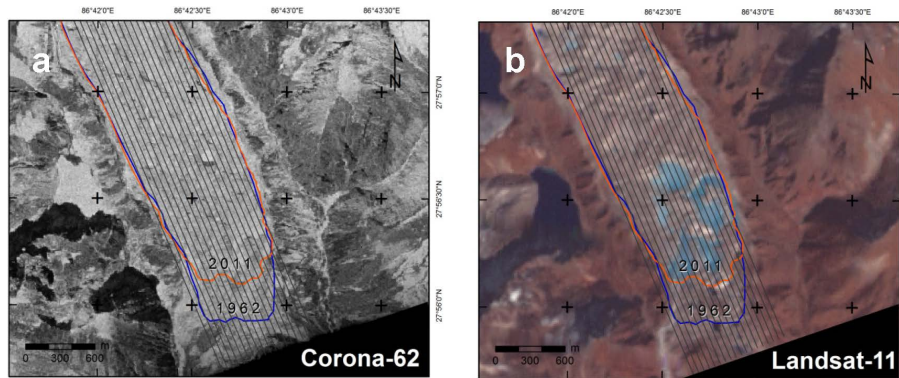


Fig. 2. Glacier delineation in **(a)** panchromatic Corona-62; **(b)** SLC-off gap filled Landsat-11. The stripes in the images are meant for mean length change calculation.

Tracing glacier changes since the 1960s

S. Thakuri et al.

Title Page

Abstract Introduction

Conclusions References

Tables Figures

⏪ ⏩

◀ ▶

Back Close

Full Screen / Esc

Printer-friendly Version

Interactive Discussion



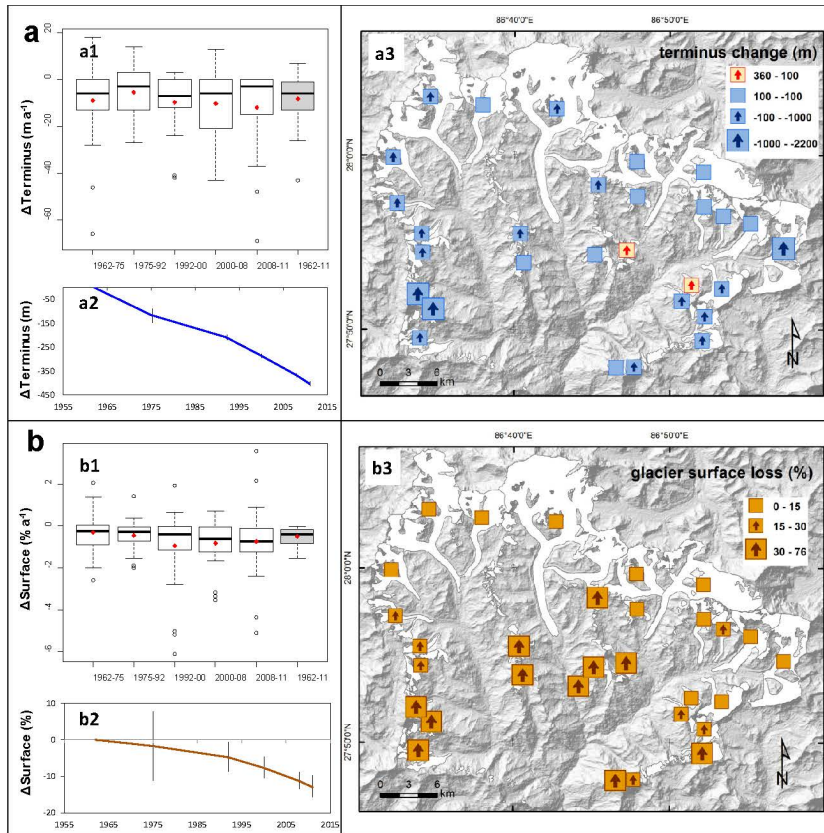


Fig. 3. Spatio-temporal changes in Mt. Everest region; **(a)** terminus position change (ΔTerm), **(b)** surface area change (ΔSurf), **(c)** shift of snow-line altitude (ΔSLA), and **(d)** debris area coverage change ($\Delta\text{DebrisCov}$). For each plot, upper left box plot represents the annual rates of change of the glaciers in the analyzed periods. The red point in the box indicates the mean. The lower left plot describes the cumulative changes with associated uncertainty. On the right side, the map represents the spatial variation of the glaciers. Figure continued on next page.

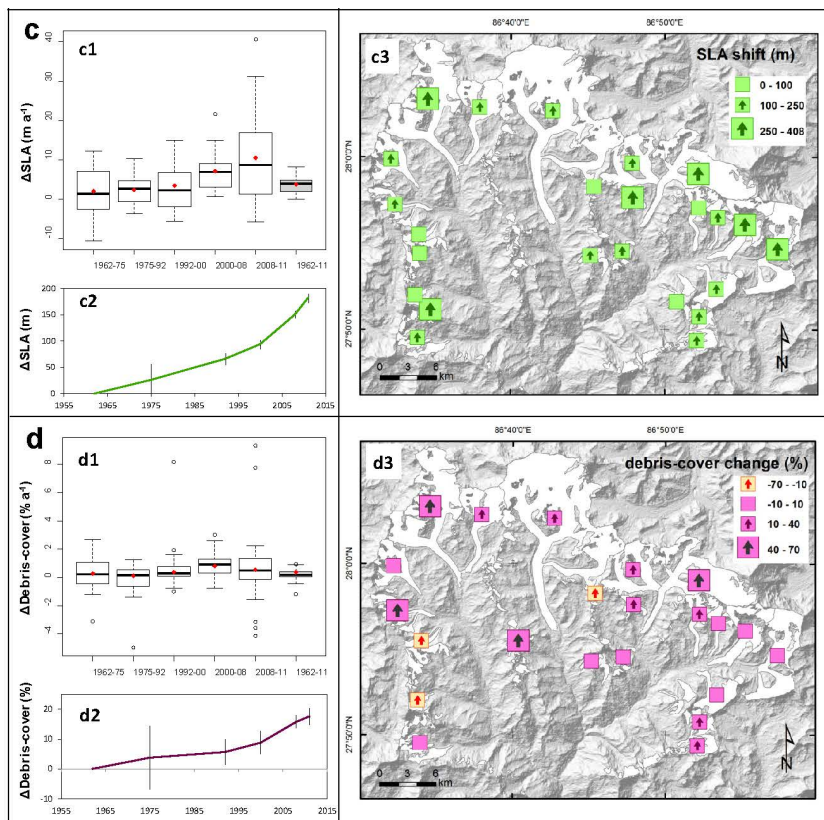


Fig. 3. Continued.

Tracing glacier changes since the 1960s

S. Thakuri et al.

Title Page

Abstract

Introduction

Conclusions

References

Tables

Figures

◀

▶

◀

▶

Back

Close

Full Screen / Esc

Printer-friendly Version

Interactive Discussion



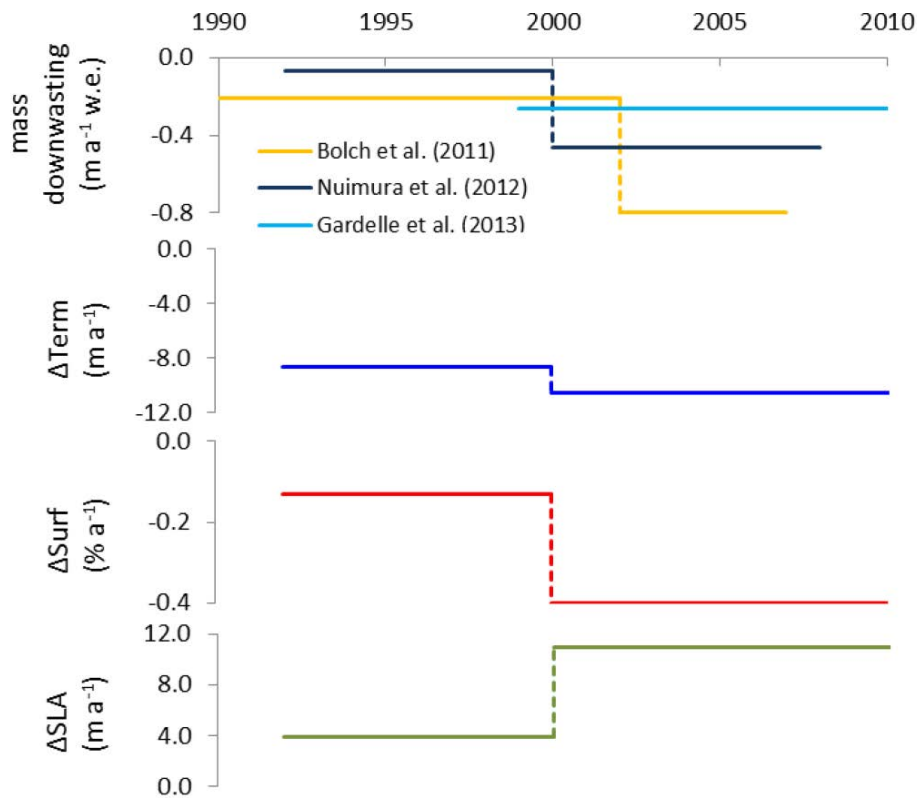


Fig. 4. Comparison for 10 selected glaciers using the terminus position change (ΔTerm), glacier surface shrinkage (ΔSurf), and shift of snow-line altitude (ΔSLA) calculated in this study and relevant mass down-wasting observations of Bolch et al. (2011), Nuimura et al. (2012). Furthermore, the mass balance data of Gardelle et al. (2013) are reported.

Tracing glacier changes since the 1960s

S. Thakuri et al.

Title Page

Abstract Introduction

Conclusions References

Tables Figures

◀ ▶

◀ ▶

Back Close

Full Screen / Esc

Printer-friendly Version

Interactive Discussion



Tracing glacier changes since the 1960s

S. Thakuri et al.

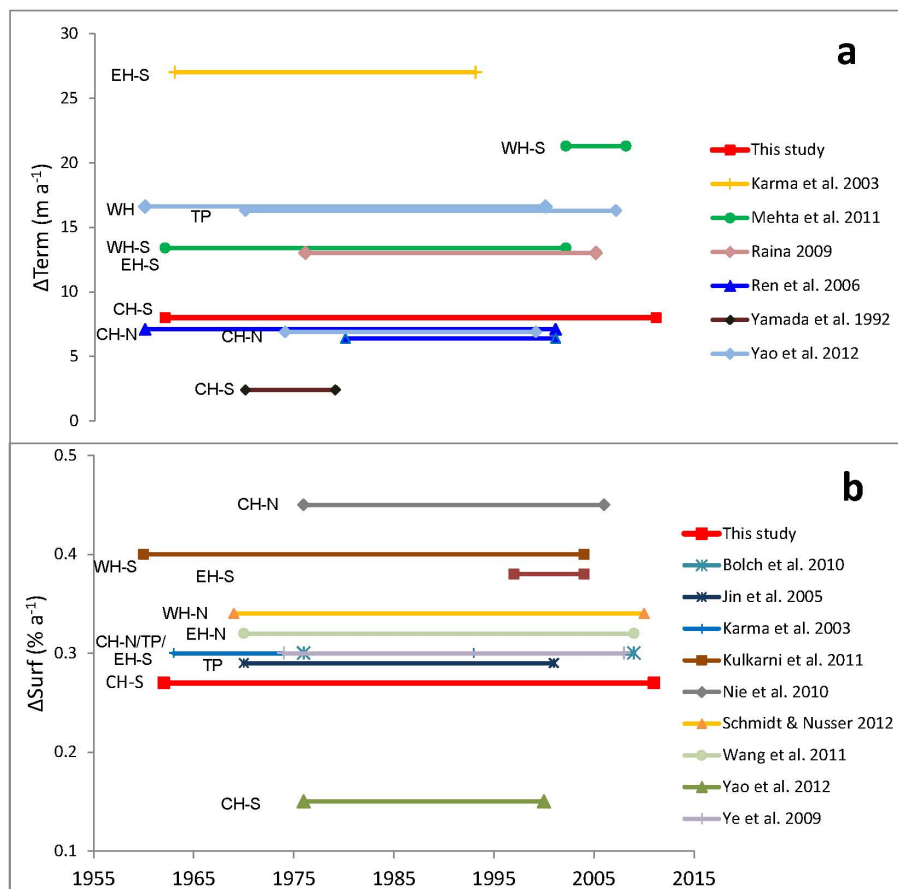


Fig. 5. Recent impact studies on Himalayan glaciers concerning both the terminus retreat **(a)** and the shrinkage **(b)**.

Title Page

Abstract Introduction

Conclusions References

Tables Figures

◀ ▶

◀ ▶

Back Close

Full Screen / Esc

Printer-friendly Version

Interactive Discussion



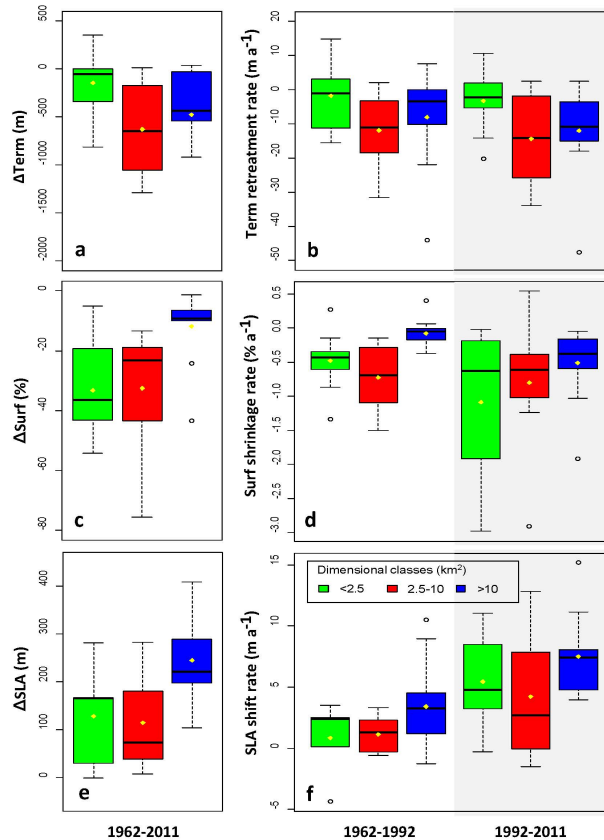


Fig. 6. Differences among three-dimensional classes of glaciers ($< 2.5 \text{ km}^2$; $2.5\text{--}10 \text{ km}^2$; $> 10 \text{ km}^2$) in terms of cumulative changes in the overall 1962–2011 period: **(a)** terminus retreat (m); **(c)** surface area shrinkage (%); **(e)** shift of SLA (m). Differences in terms of annual rate of change between 1962–1992 and 1992–2011 periods; **(b)** annual terminus retreat rate (m a^{-1}); **(d)** annual surface shrinkage rate ($\% \text{ a}^{-1}$); **(f)** shift rate of SLA (m a^{-1}).

Tracing glacier changes since the 1960s

S. Thakuri et al.

Title Page

Abstract Introduction

Conclusions References

Tables Figures

◀ ▶

◀ ▶

Back Close

Full Screen / Esc

Printer-friendly Version

Interactive Discussion

